

RESEARCH

Open Access



Preparation and purification of novel phosphatidyl prodrug and performance modulation of phosphatidyl nanoprodrug

Rui Niu, PeiLei Zhang, Feng-Qing Wang, Min Liu, QingHai Liu, Ning Jia, ShengLi Yang, XinYi Tao*
and DongZhi Wei

Abstract

Background: A novel phosphatidyl nanoprodrug system can be selectively released parent drugs in cancer cells, triggered by the local overexpression of phospholipase D (PLD). This system significantly reduces the intrinsic disadvantages of conventional chemotherapeutic drugs. However, the separation and purification processes of phosphatidyl prodrug, the precursor of phosphatidyl nanoprodrug, have not been established, and the preparation of nanocrystals with good stability and tumor-targeting capability is still challenging.

Results: In this study, we established a successive elution procedure for the phosphatidyl prodrug—phosphatidyl mitoxantrone (PMA), using an initial ten-bed volume of chloroform/methanol/glacial acetic acid/water (26/10/0.8/0.7) (v/v/v/v) followed by a five-bed volume (26/10/0.8/3), with which purity rates of 96.93% and overall yields of 50.35% of PMA were obtained. Moreover, to reduce the intrinsic disadvantages of conventional chemotherapeutic drugs, phosphatidyl nanoprodrug—PMA nanoprodrug (NP@PMA)—was prepared. To enhance their stability, nanoparticles were modified with polyethylene glycol (PEG). We found that nanoprodrugs modified by PEG (NP@PEG-PMA) were stably present in RPMI-1640 medium containing 10% FBS, compared with unmodified nanoprodrug (NP@PMA). To enhance active tumor-targeting efficiency, we modified nanoparticles with an arginine-glycine-aspartic acid (RGD) peptide (NP@RGD-PEG-PMA). *In vitro* cytotoxicity assays showed that, compared with the cytotoxicity of NP@PEG-PMA against tumor cells, that of NP@RGD-PEG-PMA was enhanced. Thus, RGD modification may serve to enhance the active tumor-targeting efficiency of a nanoprodrug, thereby increasing its cytotoxicity.

Conclusions: A process for the preparation and purification of novel phosphatidyl prodrugs was successfully established, and the nanoprodrug was modified using PEG for enhanced nanoparticle stability, and using RGD peptide for enhanced active tumor-targeting efficiency. These procedures offer considerable potential in the development of functional antitumor prodrugs.

Keywords: Phosphatidyl prodrug, Purification, Gradient elution, Silica gel column chromatography, PEGylation, RGD modification

Background

Currently, although chemotherapy is one of the main methods of cancer treatment, its use is often limited by the deleterious side effects of drug toxicity on healthy tissue encountered enroute to cancer cells (Petersen et al.

2013). As a means of resolving this problem, nanocarriers (e.g., polymeric nanoparticles) have attracted significant attention for the delivery of drugs to tumor tissues with an enhanced permeability

and retention (EPR) effect (Fang et al. 2011; Zhou et al. 2019). Liposomes, which have the advantages of biodegradability and modifiability, are the most promising and widely accepted nanocarriers (Bulbake et al. 2017; Farokhzad and Langer 2009; Andresen et al. 2005);

*Correspondence: xytao@ecust.edu.cn

State Key Laboratory of Bioreactor Engineering, Newworld Institute of Biotechnology, East China University of Science and Technology, Shanghai 200237, China

however, conventional liposome carriers typically have low drug loadings, uncontrolled encapsulation efficiencies, and significant drug burst release effects in circulation when used in vivo (Zheng et al. 2018). Low drug loading and the presence of a large number of nanocarriers may induce systemic toxicity and occasionally severe allergic reactions (Pirillo and Catapano 2015). In addition, the instability of liposomes in circulation also can result in insufficient dosages reaching the targeted cells (Zheng et al. 2018). Recently, the use of amphiphilic prodrugs, which are synthesized via chemical bonding between carriers and drugs, has emerged as a promising strategy for drug delivery (Yang et al. 2013). In contrast to the conventional drug-containing liposomes, highly efficient nanocarriers, in which the drug is directly connected with the carrier system, have been developed to facilitate nanoscale drug delivery (Lutz and Kianga 2011). Nanoscale drug delivery can overcome the drawbacks associated with the use of liposomes by increasing drug loading capacity and eliminating the premature burst release of drugs (Jain and Stylianopoulos 2010; Bildstein et al. 2011; Mura et al. 2013; Wakaskar 2018; Luo et al. 2018). The prodrug can also spontaneously self-assemble into nanoparticles (Oliyai 1996; Yang et al. 2013). Nevertheless, there are currently certain disadvantages encountered during the development of prodrugs with regard to nanoparticle stability, and efficient drug release presents a major challenge in terms of the application of nanocarrier systems. A promising strategy relating the application of nanocarriers is the exploitation of reversible bonds between carriers and small molecule drugs, which could facilitate the retention of the stability of synthesized prodrugs during storage and circulation, and also promote release at the tumor site in response to certain stimuli, such as acidic pH (Liu et al. 2019), reactive oxygen species (Luo et al. 2018), and the selective overexpression of enzymes in certain tumor tissues (Tao et al. 2017), which are related to the intrinsic characteristics of the tumor microenvironment that differ from those of normal tissues.

In a preliminary study, a novel phosphatidyl drug, which was a phosphatidyl modification of small molecule primary alcohol chemotherapeutic drugs, was synthesized via a phosphatidyl transfer reaction based on the transphosphatidylation activity of bacterial phospholipase D (PLD) on alcohol groups (Tao et al. 2017). Owing to the chemical bonding between phospholipids and drugs, this phosphatidyl nanoscale drug delivery system has the advantages of liposomal particles, while also overcoming the typical drawbacks of traditional liposomes by increasing the loading capacity of drugs and eliminating the premature burst release of drugs. In

aqueous solution, amphiphilic phosphatidyl drugs can self-assemble into nanoparticles of uniform size and selectively release parent drugs in cancer cells when triggered by the local overexpression of PLD in cancer cell. Furthermore, the prodrugs have liposome-like properties, such as modifiability, and can thus be modified, for example with polyethylene glycol (PEG) or ligands, to enhance the stability or the tumor-targeting efficiency of nanoparticles.

Ligand-mediated targeting (known as active targeting) of nanodrug has played an important role in enhancing tumor-targeting efficiency (Danhier et al. 2010) and drug delivery (Nik et al. 2019). For this purpose, various biological ligands, such as peptides (Jiang et al. 2019), antibodies (Antignani and Fitzgerald 2013; Sapra and Shor 2013; Mahmudul et al. 2018), small molecules and aptamers (Xiao et al. 2012), have been utilized as pilots to bind specific receptors or surface molecules that are overexpressed in tumor cells (Jiang et al. 2019). This approach has facilitated heightened selectivity between tumor and normal cells. Among these ligands, the arginine-glycine-aspartic acid (RGD) peptide, which recognizes the $\alpha\beta 3$ integrin receptor that is overexpressed in various human cancers cells (Jiang et al. 2019), is regarded as a particularly effective targeting agent (Keer et al. 1990; Shi et al. 2015) and is considered ideal for this purpose based on its defined structure and small molecular weight.

Mitoxantrone (Novantrone[®]), a synthetic anthracenedione derivative, is an antineoplastic, immunomodulatory agent and has effect on acute leukemias, advanced breast cancer, multiple myeloma, and non-Hodgkin's lymphoma (Faulds et al. 1991). The antibiotic antitumor agent mitoxantrone (MIT) can block the synthesis and transcription of DNA and interfere in the synthesis of RNA to kill tumor cells (Wang et al. 2018).

Phosphatidyl prodrugs, which have been shown to have excellent antitumor activity in vivo and significantly reduce the intrinsic disadvantages of traditionally used chemotherapeutic drugs, offer considerable potential in the development of functional antitumor prodrugs with promising therapeutic clinical applications (Tao et al. 2017). In the present study, with a view toward pre-clinical application studies of phosphatidyl prodrugs, we examined the preparation and purification of phosphatidyl prodrugs and sought to undertake pilot-scale production. We developed a multi-stage phosphatidyl prodrug system functionalized with RGD and PEG, and evaluated the characteristics of the actively targeted prodrug in terms of physicochemical properties, drug release kinetics, and in vitro cytotoxicity. The findings of this study will lay the foundations for future therapeutic clinical applications of phosphatidyl prodrugs.

Materials and methods

Materials

Mitoxantrone HCl ($C_{22}H_{30}Cl_2N_4O_6$, 98%, MW = 517.41) was purchased from Shifeng Biological Technology Co. Ltd (Shanghai, China); and the Cell Counting Kit-8 (CCK-8) was purchased from Yeasen Biological Technology Co. Ltd (Shanghai, China). Chloroform, methanol, *n*-hexane, isopropyl alcohol, *n*-heptane, glacial acetic acid, and glass column were purchased from Titan Biological Technology Co. Ltd (Shanghai, China). DSPE-mPEG2000 was purchased from Ponsure Biological Technology Co. Ltd (Shanghai, China). CRGDyC was purchased from Apeptide Co., Ltd (Shanghai, China). Silica gel was purchased from Jiangyou Silica Gel Development Co., Ltd (Shanghai, China). RPMI-1640 medium was purchased from Hyclone (America). FES was purchased from Gemini (America, Cat: 900-108).

Cell lines and cell culture

The human breast cancer cell lines MCF-7 were purchased from the Cell Bank at the Chinese Academy of Sciences (Shanghai, China) and were originally imported from ATCC (USA). The cell lines were cultured in Roswell Park Memorial Institute (RPMI) 1640 medium (HyClone) supplemented with 10% fetal bovine serum (FBS), 100 U/mL penicillin, and 100 µg/mL streptomycin and incubated in an incubator at 5% carbon dioxide and 37 °C.

chromatography (TLC) and detected using electron spray ionization (ESI) high-resolution time-of-flight mass spectrometry.

For the purposes of the large-scale preparation of PMA, we performed purification using silica gel column chromatography (SGCC). A glass column (19# G3: L × i.d.: 45 cm × 2 cm) was prepared by wet packing with a slurry of silica gel (300–400 mesh). Prior to sample loading, the column was washed with the mobile phase (200 mL). The gradient elution system used for chromatographic separation consisted of a mixture of chloroform, methanol, glacial acetic acid, and water. The sample dissolved in *n*-hexane and the silica gel was stirred evenly and dried overnight for dry loading. The mobile phase was run through the column by gravity and pressure, and 10-mL fractions were subsequently collected. Each fraction was assayed by TLC to determine the fraction(s) containing the target compound. After purification, the recovery and purity of PMA were quantified using an HPLC system comprising an Agilent ultraviolet detector (243 nm; Agilent, USA) and a KR100-5SIL 250 × 4.6 mm column. The mobile phase used for analysis contained 18% phosphoric acid in a mixture of methanol and acetonitrile (62.8:37.2 v/v) and was applied at a flow rate of 1.0 mL/min. All analyses were carried out in triplicate.

$$\text{Recovery (\%)} = \frac{\text{quantity of PMA after SGCC (mg)}}{\text{quantity of PMA in PCE (mg)}} * 100\%$$

$$\text{Purity (\%)} = \frac{\text{concentration of PMA (mg/ml)}}{\text{concentration of PC (mg/ml)} + \text{concentration of PMA (mg/ml)}} * 100\%.$$

Synthesis of PMA

The enzymatic synthesis of PMA was carried out in a two-phase system as described by Hirche et al. (Hirche et al. 1997). PC (50 mM) was dissolved in *n*-heptane (5 mL) to initiate the reaction. Subsequently, MA (85 mM) was added to 200 mM sodium acetate buffer (80 mM CaCl₂, pH 5.6) and isopropyl alcohol (1 mL). The above two solutions were sonicated at 45 °C for 2 h, then 5U PLD was added, The reaction was carried out in an orbital shaker incubator at 45 °C under 220 rpm for 2 h.

Purification of PMA via silica gel column chromatography

On the basis of the polarity of PMA, the crude extract of PMA (PCE) was extracted with *n*-hexane to obtain a mixed solution containing PMA, PC, MA, and impurities. Given that the PMA and impurities have similar polarities in the extract, organic solvent extraction could not be used to separate the substrate products. However, PMA samples can be obtained via thin-layer

Purification amplification of PMA

Column chromatography process flow refers to purification of PMA via silica gel column chromatography. A glass column (19# G3: L × i.d.: 45 cm × 8 cm) was prepared.

Synthesis of DSPE-PEG2000-RGD

DSPE-PEG2000-RGD was synthesized according to (Xiang et al. 2013; Yang et al. 2014), with slight modifications. Briefly, cysteine-modified RGD (6.8 mg) was dissolved in 4.5 mL of HEPES buffer (20 mM HEPES, 10 mM EDTA-Na₂, pH 6.5). 0.30 mg DSPE-PEG2000-Mal was hydrated in the HEPES buffer and added drop-wise to RGD peptide solutions with low-speed agitator at room temperature under nitrogen protection. After 48 h of stirring, L-cysteine (10 times the molar ratio to maleimide residues) was added for capping unreacted maleimide group stirring. After another 4 h of stirring, the excess peptides and quencher were removed by

dialyzing the reaction mixture with a molecular weight cutoff (MWCO) of 3000 against distilled water for 48 h. The solution was lyophilized and stored at 4 °C. The final resulting DSPE–PEG2000–RGD was confirmed using MALDI-TOF MS.

Preparation and characterization of nanoparticles

Three types of liposomal formulations were prepared.

Synthesis and characterization of NP@PMA

Owing to the amphipathic nature of PMA, the prodrug can form nanoparticles in water via self-assembly, which in the present study were prepared using an emulsion method. PMA (10 mg) was dissolved in tetrahydrofuran (2 mL) and slowly added dropwise to water (5 mL). Following continuous stirring for 2 h at room temperature, the particle size and size distribution of the NP@PMA were measured using a granulometer (Malvern, UK). Morphological analyses of the NP@PMA particles were conducted using transmission electron microscopy (TEM) (JEOL, Japan).

Synthesis and characterization of NP@PEG–PMA and NP@RGD–PEG–PMA

Owing to the liposome-like nature of NP@PMA, the prodrug can be modified by PEG and active targeting substances. The NP@ PEG–PMA were prepared with an emulsion method using NP@ PMA. PMA (10 mg) and DSPE-mPEG (1.84 mg) were dissolved in tetrahydrofuran (2 mL) and slowly added dropwise to water (5 mL). The NP@ RGD–PEG–PMA was prepared with an emulsion method. PMA (10 mg), DSPE-mPEG (1.52 mg), and DSPE–PEG–RGD (0.38 mg) were dissolved in tetrahydrofuran (2 mL) and slowly added dropwise to water (5 mL). The next process is similar to the synthesis and characterization of NP@PMA.

Nanoparticles release in vitro

The release of MA from NP@PMA, NP@PEG–PMA, and NP@RGD–PEG–PMA was measured by HPLC on Agilent 1200 (Agilent Technologies Inc., Shanghai Branch) and Zorbax Eclipse XDB-C18 column (5 μm, 4.6 mm × 250 mm) at room temperature. Briefly, PMA (1 mg) was subjected to enzymolysis with PLD (10 U) dissolved in saline (1 mL) at 37 °C for 2 h; Three samples(50 μL) were taken for 0 h, 1 h, 3 h, 6 h, and 24 h. After 24 h, the MA release was assessed by HPLC with injection of 10 μL. The mobile phase used for analysis was water containing 29.1 mM C₇H₁₅NaO₃S and 0.88% acetic acid (v %)/CH₃CN (70:30, v/v). The eluates from the column outlet were continuously monitored by a UV detector at 254 nm. All analyses were performed in triplicate.

In vitro nanoparticle cytotoxicity assays

MCF-7 cells were seeded in 96-well plates at a density of 3000 cells per well. After overnight incubation, the medium was replaced by fresh medium, to which free MA, NP@PMA, NP@PEG–PMA, and NP@RGD–PEG–PMA were added. The final concentration of MA was 7 μM, 3.5 μM, 1.75 μM, 0.875 μM, 0.4375 μM, and 0.21875 μM. The final concentration of PMA was 56 μM, 28 μM, 14 μM, 7 μM, and 3.5 μM. After 72 h incubation, MCF-7 cells were treated with CCK-8 (10 μL per well) and incubated for 4 h. Quantification analysis was performed at 450 nm by a Multiscan Spectrum (BioTek Instruments, Inc. USA).

Results and discussion

Successful synthesis of PMA

The mitoxantrone that contains primary alcohol groups can be readily transferred by phosphatidylcholine via phospholipase (PLD) (Fig. 1a).

As shown in Fig. 1b, a crude extract of PMA (PCE), which included MA, PMA, PC, and impurities, was obtained following extraction. The concentration of PMA reached a maximum at 4.7 min, as validated by the corresponding standard (Fig. 1d, e). The content of PMA in PCE was 45.1%, measured by HPLC. PMA was separated from PCE by TLC and detected by ESI high-resolution time-of-flight mass spectrometry. A major peak was observed at 1123.67 (indicated by the red box in Fig. 1c). Mass–charge ratios indicated that the mean MW of PMA (1123.67) was consistent with the calculated mean MW (1122.48) of the corresponding product.

Successful purification of PMA

As shown in Fig. 1b, high concentrations of MA, PC, and impurities were present in the PCE. To enhance separation efficiency, we used silica gel chromatography (SGCC). To achieve optimal separation, we examined the effects of different chromatographic parameters on separation efficiency, including the ratio of sample to adsorbent and mobile phase composition.

The target components could be enriched in different elution fractions due to the different polarities of the eluent solvents used in SGCC (Wu et al. 2015). For obtaining high-purity PMA from the PCE, we used SGCC based on the developing solvent system used for TLC. As shown in Table 1, the impurities were dispersed in the low-polarity eluent. In the eluent (chloroform/methanol/glacial acetic acid/water = 26/10/0.8/1.5), the PMA could be partially isolated from the impurities and PC by continuous elution, and we accordingly obtained PMA of 94.71% purity, with a recovery rate of slightly less than 23.52%, which can be attributed to the partial overlap of PMA and the impurities in fractions. On further increasing the

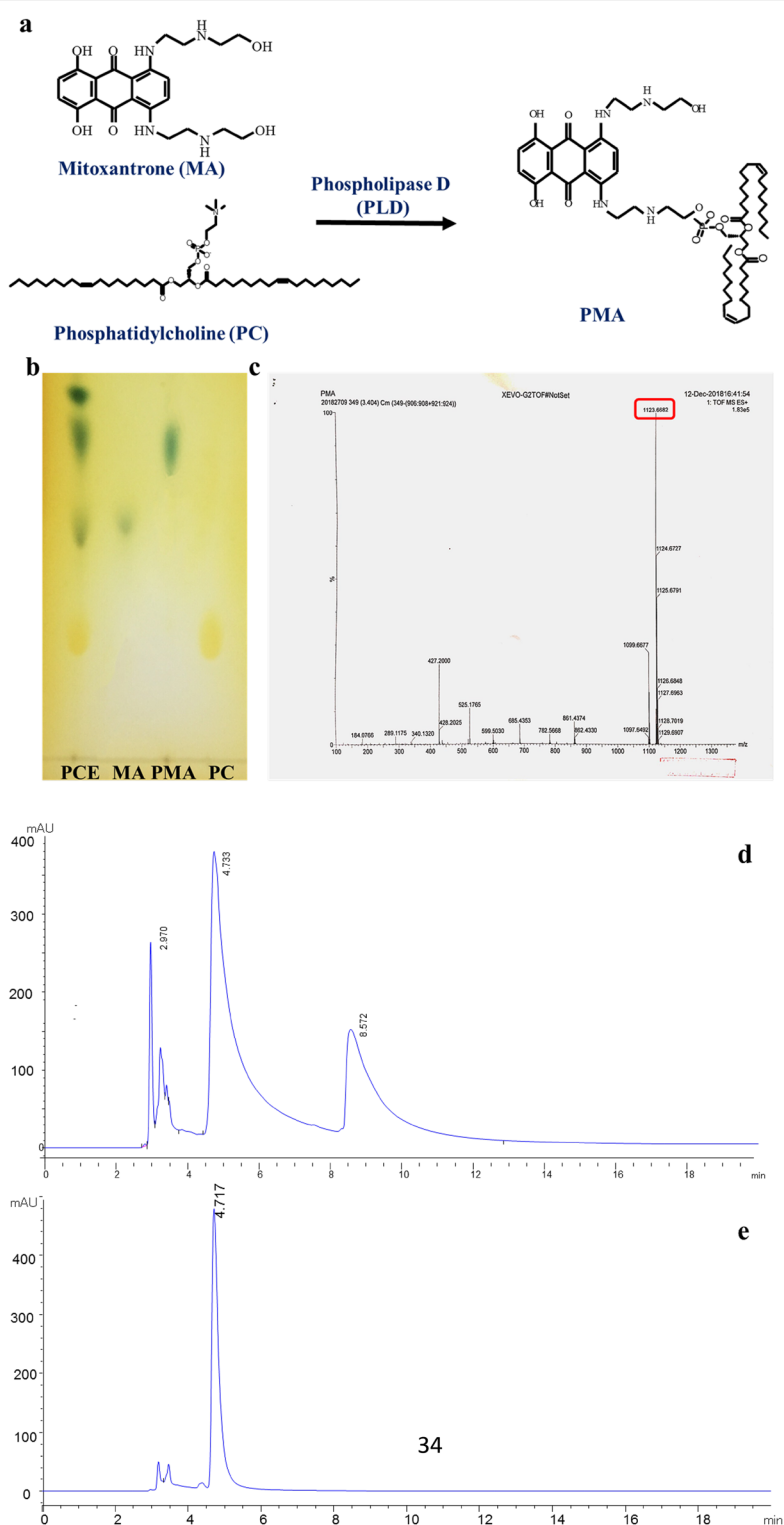


Fig. 1 Synthesis and characterization of PMA. **a** Scheme of the synthesis of PMA; **b** thin-layer chromatography analysis of a crude extract of PMA (PCE), mitoxantrone (MA), (phosphatidyl mitoxantrone) PMA, and phosphatidylcholine; (PC); **c** MS analysis: electron spray ionization analysis of PMA; **d** HPLC chromatograms of crude extract of PMA (PCE); **e** HPLC chromatograms of PMA

Table 1 Different eluent compositions

Eluent compositions	Recovery (%)	Purity (%)
Chloroform/methanol/glacial acetic acid/water = 26/10/0.8/0.7 (v/v/v/v)	N/A ^a	
Chloroform/methanol/glacial acetic acid/water = 26/10/0.8/1.1 (v/v/v/v)	N/A ^a	
Chloroform/methanol/glacial acetic acid/water = 26/10/0.8/1.5 (v/v/v/v)	23.52 ± 0.02	94.71 ± 3.64
Chloroform/methanol/glacial acetic acid/water = 26/10/0.8/3 (v/v/v/v)	N/A ^b	

^a N/A, not available. Owing to the low polarity of the eluent, PMA could not be eluted

^b N/A, not available. Because separation of PMA from the impurities and PC was not achieved

Table 2 Different gradient eluent conditions (quantitative analysis by HPLC, flow rate = 3.5 mL/min)

Gradient eluent system	Time (min)	The composition ratio of eluent (Chloroform/methanol/glacial acetic acid/water) (v/v/v/v)	Recovery (%)	Purity (%)
1	0	26/10/0.8/0.7	36.75 ± 0.03	96.06 ± 2.18
	100	26/10/0.8/2		
	160	End		
2	0	26/10/0.8/0.7	38.62 ± 0.02	93.97 ± 2.13
	100	26/10/0.8/2		
	120	26/10/0.8/3		
	160	End		
3	0	26/10/0.8/0.7	50.35 ± 0.02	96.93 ± 1.9
	100	26/10/0.8/3		
	150	End		
4	0	26/10/0.8/1.1	68.25 ± 0.03	69.02 ± 2.25
	20	26/10/0.8/3		
	70	End		

proportion of water in the eluent (26/10/0.8/3), PMA was unable to separate from the impurities and PC due to the complete overlap of their elution peaks.

The aforementioned results illustrate that separation using a single eluent is not an ideal method for the separation of PMA from PC and impurities, and therefore we opted to use gradient elution to maximize the separation of PMA from other components of the crude extract.

When using SGCC, different components in samples can be enriched in different elution fractions due to differences in the polarity of the solvents comprising the eluent (Wu et al. 2015), and on the basis of this principle, we used gradient elution separation to obtain high-purity target products. For SGCC separation, we examined the efficacy of four gradient eluent conditions, all of which facilitated the separation of PMA from the impurities. A successive elution procedure was thus established comprising an initial elution with a ten-bed volume of chloroform/methanol/glacial acetic acid/water (26/10/0.8/0.7) followed by elution with a five-bed volume of chloroform/methanol/glacial acetic acid/water (26/10/0.8/3). As shown in Table 2, using these gradient elution conditions, the purity of PMA obtained was 96.93%, and the recovery rate increased to 50.35% compared with the 23.52% achieved when using a single eluent.

The recovery yield increases with an increase in loading amount, but as it exceeds the column loading capacity, the recovery yield decreases, which means the separation efficiency of silica gel columns decreases (Zhang et al. 2012). The loading amount is denoted by the proportion of sample to adsorbent (the weight of PMA in PCE/the weight of silica gel in this test). If the proportion of sample to adsorbent is greater than 10 mg/g (Table 3), this would lead to overload. Normally, separation efficiency will decrease concomitant with an increase in the ratio of sample to adsorbent, due a reduction in the available interaction surface area (Melwita et al. 2011). The results shown in Table 3 indicate that the optimal loading amount on the silica gel column was 10 mg/g, which gave a recovery of 44.02% ± 0.02%.

Table 3 The effect of different sample to adsorbent ratios on PMA recovery and yield

Ratio of sample to adsorbent (mg/g)	Recovery rate (%)
6.7	50.35 ± 0.02
10	44.02 ± 0.02
13.3	28.77 ± 0.01

A successive amplification procedure was established by initially eluting with a ten-bed volume of chloroform:methanol:glacial acetic acid:water (26/10/0.8/0.7) followed by elution with a five-bed volume of chloroform:methanol:glacial acetic acid:water (26/10/0.8/3). In a single PMA purification procedure with a loading of 8.89 mg/g, a PMA recovery yield and recovery rate of 593 mg and 46.33% were achieved, respectively.

Synthesis of DSPE–PEG2000–RGD

The synthesis of DSPE–PEG2000–RGD was executed according to the scheme depicted in Fig. 2a.

DSPE–PEG2000–RGD was synthesized via the thiol–ene “click” reaction of the sulphydryl group of RGD peptide with the maleimide group indicated in Fig. 3a. The major peak at 3490.8 (Fig. 2b, marked by number) mass–charge ratios verified that the mean MW of RGD–PEG2000–DSPE was 3490.8, which was in agreement with the calculated mean MW (3493.6) of the corresponding product.

Preparation and characterization of nanoparticle formulation

PEGylation can lead to a shielding of nanoparticles from immunological recognition and from loss of stability, as it can promote the development of a steric barrier between the biological medium and the liposomal surface (Sangrà et al. 2017). As a consequence of PEGylation, surface–surface interactions, including the aggregation of nanoparticles and adsorption of plasma proteins, are reduced (Dos Santos et al. 2007). Given that the arginine–glycine–aspartate (RGD) triad shows a strong affinity and selectivity for the $\alpha v\beta 3$ integrin that is overexpressed in malignant tissues, it has been used extensively in nanoparticle targeting (Sangrà et al. 2017).

Accordingly, in the present study, we modified the synthesized nanodrug using PEG and RGD to, respectively, enhance nanoparticle stability and increase active tumor-targeting efficiency. As the different physicochemical characteristics of nanoparticle can have differing effects on therapeutic performance, it is accordingly essential to measure the sizes and the surface potentials of nanoparticles (Mu and Feng 2002). The physicochemical characteristics of the NP@PMA, NP@PEG–PMA, and NP@RGD–PEG–PMA nanoparticles prepared in the present study are summarized in Table 4. As shown in the table, the size of the NP@PMA particles was 149.1 ± 0.14 nm, whereas that of the NP@PEG–PMA and NP@RGD–PEG–PMA particles was 115.2 ± 1.84 nm and 125.2 ± 1.27 nm, respectively. All three nanoparticle types exhibited a narrow range of size distribution (polydispersity index = 0.2). The zeta potential values for the NP@PMA, NP@PEG–PMA, and NP@RGD–PEG–PMA

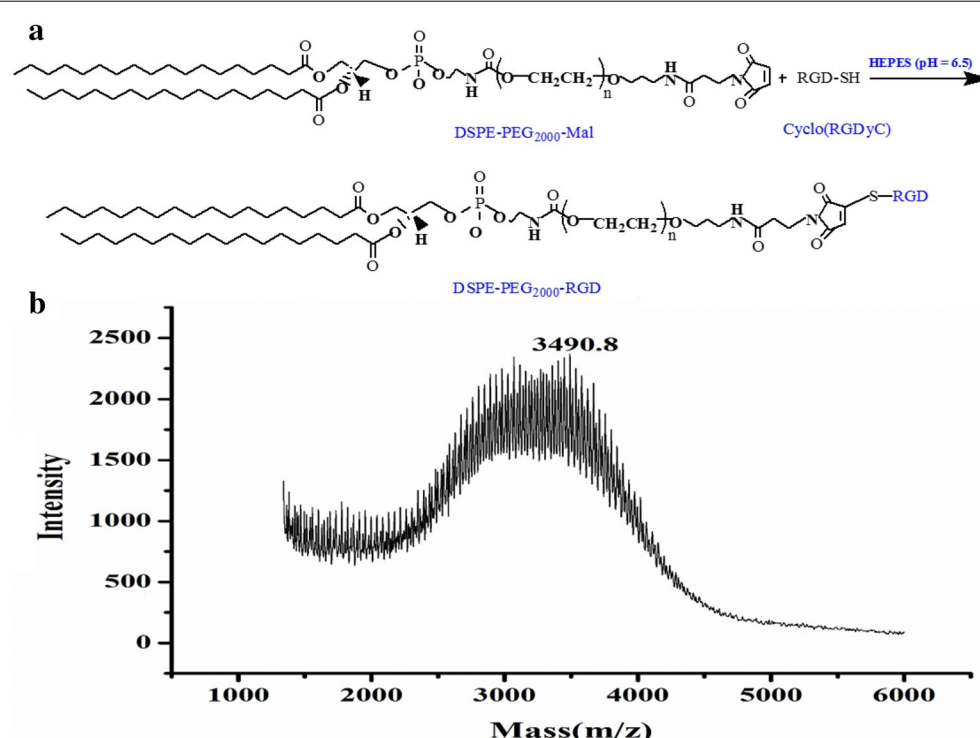
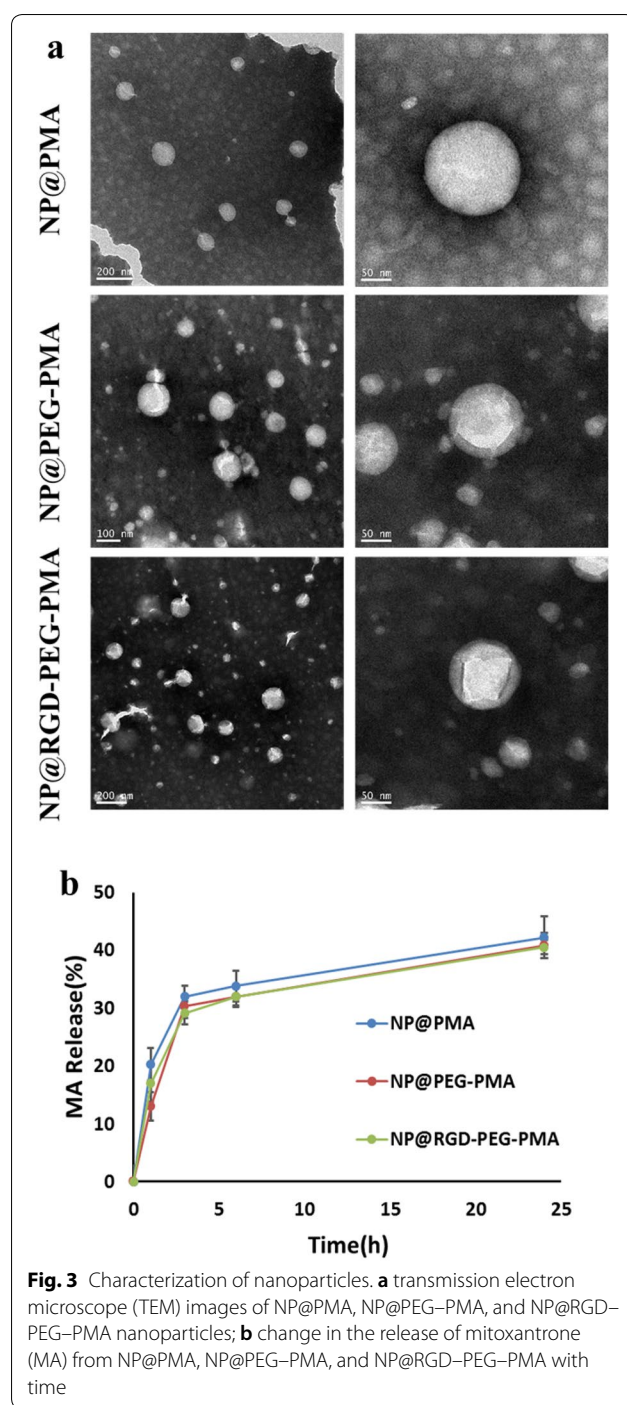


Fig. 2 Synthesis of RGD–PEG2000–DSPE. **a** scheme of the synthesis of RGD–PEG2000–DSPE; **b** MALDI–TOF mass spectra of the synthesized RGD–PEG2000–DSPE conjugate



particles were 41.7 ± 0.42 , 29.8 ± 2.4 , and 33.7 ± 0.51 mV, respectively. Each of the three nanoparticle types had a uniform spherical shape and did not aggregate under physiological conditions (Fig. 3a).

To evaluate the effect of different modifications on the drug release of the phosphatidyl prodrugs, we examined the in vitro enzymatic-induced release of MA from different nanocrystals (Fig. 3b). There was no significant difference among the different nanocrystals with respect to MA release, thereby indicating that PEG and RGD modifications have no apparent effects on the enzymatic hydrolysis of PMA in vitro.

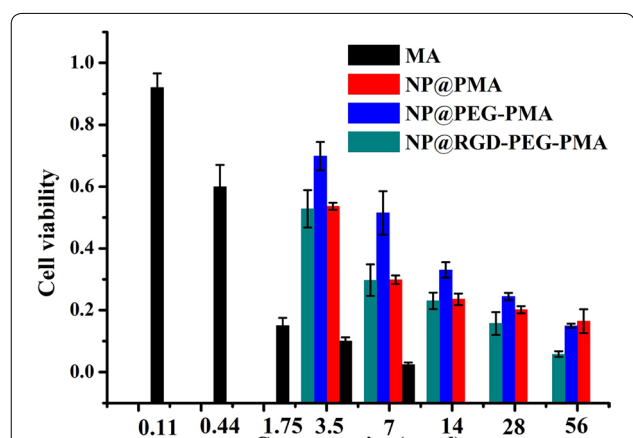
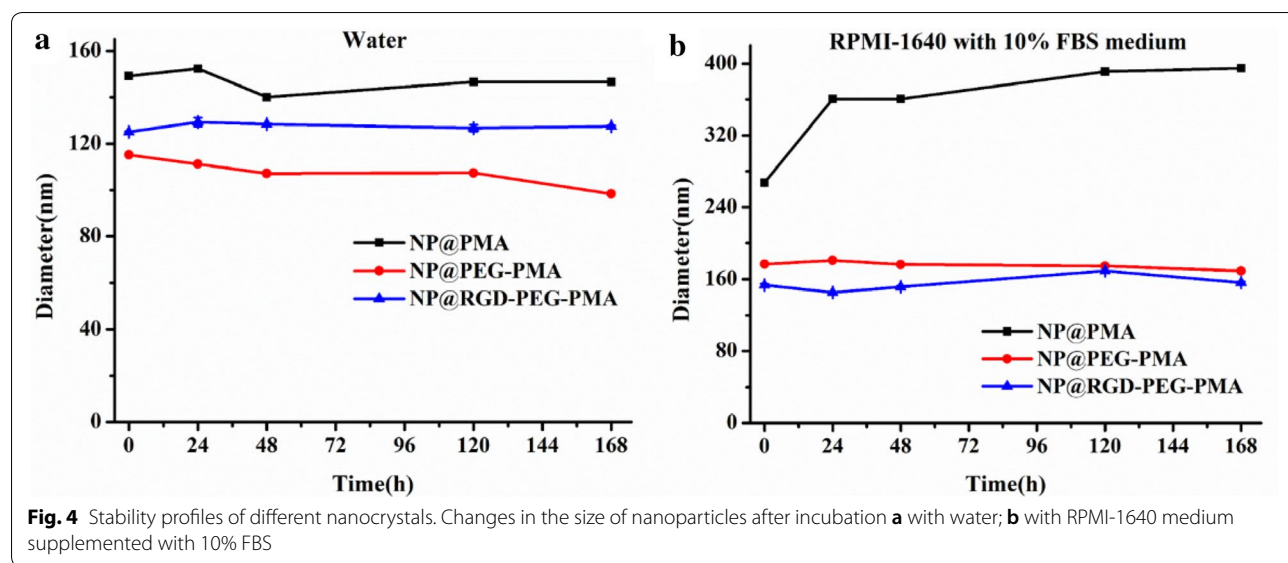
Investigation of the in vitro stability of the different nanocrystals showed that the size of PEG-modified nanoparticle (NP@PMA-PEG and NP@PMA-PEG-RGD) remained at approximately 120 nm in water and 160 nm in RPMI-1640 medium containing 10% FBS within a 168-h incubation period (Fig. 4a, b). In contrast, although the average size of unmodified nanoparticles (NP@PMA) remained at approximately 150 nm in water within 168 h, they had increased to approximately 400 nm after a 168-h incubation in RPMI-1640 medium containing 10% FBS. Therefore, we concluded that the particle size of PEG-modified nanoparticle (NP@PEG-PMA and NP@RGD-PEG-PMA) could remain unchanged in water and RPMI-1640 medium containing 10% FBS; however, unmodified nanoparticle could remain stable in water and became larger in RPMI-1640 medium containing 10% FBS. The result that modified nanoparticles remained stable in two solutions, whereas unmodified nanoparticles were not stable in a medium indicated that the unmodified nanoparticle underwent aggregation of nanocrystals in this medium. We speculate that the substantial increase in the average size of NP@PMA in this medium is perhaps related to the adhesion between serum protein molecules and the PMA layer (Ku et al. 2010). In contrast, the average size of the PEGylated nanoparticles remained unchanged in the medium for 168 h, which can probably be attributed to PEG modification having a protective effect on the PMA layer, and thereby preventing adhesion with serum protein molecules (Ku et al. 2010). This in turn indicates the superiority of NP@PMA-PEG and NP@PMA-PEG-RGD with respect to plasma stability.

In vitro cytotoxicity assays

The cytotoxicity of the NP@PMA, NP@PEG-PMA, and NP@RGD-PEG-PMA prodrugs was investigated to evaluate the effect of PEGylation and RGD modification on the cytotoxicity of the phosphatidyl prodrugs. As shown in Fig. 5, NP@PMA, NP@PEG-PMA, and NP@RGD-PEG-PMA all had a cytotoxic effect on the tumor cells. The IC₅₀ (0.55 μM) of free MA was lower

Table 4 Physicochemical properties of nanoparticles

Nanoparticles	Diameter (nm)	PDI	Zeta potential (mV)
NP@PMA	149.1 ± 0.14	0.198 ± 0.013	41.7 ± 0.42
NP@PEG-PMA	115.2 ± 1.84	0.227 ± 0.001	29.8 ± 2.4
NP@RGD-PEG-PMA	125.2 ± 1.27	0.205 ± 0.002	33.7 ± 0.51



than nanoparticles, because the small molecule drugs was effects on tumor cell directly and killing them, nanodrugs need to be released in tumor cells and effects on tumor cell. The release process of nanodrug was slow. Nevertheless, the nanodrug may show its advantageous effects (such as EPR) in the body. Moreover, comparison of the cytotoxicity of these three nanodrugs revealed that the cytotoxicity of NP@PEG-PMA ($IC_{50}=7.8 \mu M$) against the MCF-7 cells was lower than that of NP@PMA ($IC_{50}=4.1 \mu M$), which could be attributed to a reduced electrostatic attraction between the PEGylated nanoprodrug and the cell plasma membrane, resulting in a less efficient uptake (Majzoub et al. 2014). Compared with

the cytotoxicity of NP@PEG-PMA against the tumor cells, that of NP@RGD-PEG-PMA ($IC_{50}=3.7 \mu M$) was observed to be enhanced. In this case, we speculate that overexpression of the $\alpha v\beta 3$ integrin receptor on MCF-7 cells may have mediated the endocytosis of NP@RGD-PEG-PMA, which may thus have enhanced the cellular uptake of the prodrug resulting in an increased cytotoxicity against the cancer cells (Zhou et al. 2017). Thus, this study indicate that the PEG modification performed in the present study may contribute to solving the problem of nanoparticle stability, whereas RGD modification may serve to enhance the active tumor-targeting efficiency of the nanoprodrug, thereby increasing its cytotoxicity against cancer cells.

Conclusion

In previous studies, a phosphatidyl prodrug was established that offers considerable potential for the development of functional antitumor prodrugs with promising therapeutic clinical applications. In the present study, a preparation and purification procedure for a novel phosphatidyl prodrug (PMA) was established, which enabled to obtain target substance PMA, with 96.93% purity and a recovery of 50.35%. The results of PMA separation amplification experiment show that single-separation pilot-scale yields of PMA can approximately reach 600 mg. Moreover, PEG modification contributed to solving the problem of nanoparticle stability. PEG modification was, however, observed to reduce prodrug antitumor activity. Nevertheless, this problem could be circumvented by modification with an RGD peptide, which facilitated the active targeting of the NP@RGD-PRG-PMA against cancer cells. Thus, a nanoscale drug delivery system was

established and succeeded in having increased stability of the nanoparticles, prolonged circulation, and enhanced active tumor-targeting efficiency.

Abbreviations

PMA: phosphatidyl mitoxantrone; DSPE-mPEG2000: 1,2-distearoyl-sn-glycero-3-phosphoethanolamine-N-[methoxy(polyethylene glycol)-2000]; DSPE-PEG2000-MAL: 1,2-distearoyl-sn-glycero-3-phosphoethanolamine-N-[maleimide(polyethyleneglycol)-2000]; CRGDyC: cyclo (Arg-Gly-Asp-D-Tyr-Cys); WST-8: (2-(2-methoxy-4-nitrophenyl)-3-(4-nitrophenyl)-5-(2,4-disulfonylphenyl)-2H-tetrazolium, monosodium salt); TLC: thin-layer chromatography; UV: ultraviolet; HPLC: high-performance liquid chromatography; SGCC: silica gel column chromatography; HEPES: 4-(2-hydroxyethyl)-1-piperazineethanesulfonic acid; EDTA-Na₂: ethylenediaminetetraacetic acid disodium salt; MW: molecular weight; U: active unit; SGCC: silica gel column chromatography; PCE: PMA crude extract; FBS: fetal bovine serum.

Acknowledgements

We sincerely thank the Cell Bank at the Chinese Academy of Sciences for providing the MCF-7 cell lines.

Authors' contributions

RN performed the research experiments and wrote the manuscript. PLZ and NJ helped in the experiments. XYT directed the study as tutors. ML, FQW, QHL, SLY, and DZW guided both authors during the experiments and manuscript preparation. All authors read and approved the final manuscript.

Funding

This work was financially supported by the National Natural Science Foundation of China (Grant No. 81603056) and by the Open Funding Project of the State Key Laboratory of Bioreactor Engineering.

Availability of data and materials

All data generated or analyzed in this study are included in the paper.

Ethics approval and consent to participate

Not applicable.

Consent for publication

Not applicable.

Competing interests

The authors declare that they have no competing interests.

Received: 4 July 2019 Accepted: 16 October 2019

Published online: 01 November 2019

References

- Andresen TL, Jensen SS, Jørgensen K (2005) Advanced strategies in liposomal cancer therapy: problems and prospects of active and tumor specific drug release. *Prog Lipid Res* 44:68–97
- Antignani A, Fitzgerald D (2013) Immunotoxins: the role of the toxin. *Toxins* 5:1486–1502
- Bildstein L, Dubernet C, Couvreur P (2011) Prodrug-based intracellular delivery of anticancer agents. *Adv Drug Deliv Rev* 63:3–23
- Bulbake U, Doppalapudi S, Kommineni N, Khan W (2017) Liposomal formulations in clinical use: an updated review. *Pharm* 9:12
- Danhier F, Feron O, Préat V (2010) To exploit the tumor microenvironment: passive and active tumor targeting of nanocarriers for anti-cancer drug delivery. *J. Control Release* 148:135–146
- Dos Santos N, Allen C, Doppen A-M, Anantha M, Cox KAK, Gallagher RC, Karlsson G, Edwards K, Kenner G, Samuels L, Webb MS, Bally MB (2007) Influence of poly(ethylene glycol) grafting density and polymer length on liposomes: relating plasma circulation lifetimes to protein binding. *Biochim Biophys Acta Biomembr* 1768:1367–1377
- Fang J, Nakamura H, Maeda H (2011) The EPR effect: unique features of tumor blood vessels for drug delivery, factors involved, and limitations and augmentation of the effect. *Adv Drug Deliver Rev* 63:136–151
- Farokhzad OC, Langer R (2009) Impact of nanotechnology on drug delivery. *ACS Nano* 3:16–20
- Faulds D, Balfour JA, Chrisp P, Langtry HD (1991) Mitoxantrone. *Drugs* 41:400–449
- Hirche F, Koch MHJ, König S, Wadewitz T, Ulbrich-Hofmann R (1997) The influence of organic solvents on phospholipid transformations by phospholipase D in emulsion systems. *Enzyme Microb Technol* 20:453–461
- Jain RK, Stylianopoulos T (2010) Delivering nanomedicine to solid tumors. *Nat Rev Clin Oncol* 7:653–664
- Jiang Z, Guan J, Qian J, Zhan C (2019) Peptide ligand-mediated targeted drug delivery of nanomedicines. *Biomater Sci* 7(2):461–471. <https://doi.org/10.1039/C8BM01340C>
- Keer HN, Kozlowski JM, Tsai YC, Lee C, McEwan RN, Grayhack JT (1990) Elevated transferrin receptor content in human prostate cancer cell lines assessed in vitro and in vivo. *J Urol* 143:381–385
- Ku SH, Ryu J, Hong SK, Lee H, Park CB (2010) General functionalization route for cell adhesion on non-wetting surfaces. *Biomaterials* 31:2535–2541
- Liu B-Y, Yang X-L, Xing X, Li J, Liu Y-H, Wang N, Yu X-Q (2019) Trackable water-soluble prodrug micelles capable of rapid mitochondrial-targeting and alkaline pH-responsive drug release for highly improved anticancer efficacy. *ACS Macro Lett* 8:719–723
- Luo C-Q, Zhou Y-X, Zhou T-J, Xing L, Cui P-F, Sun M, Jin L, Lu N, Jiang H-L (2018) Reactive oxygen species-responsive nanoprodug with quinone methides-mediated GSH depletion for improved chlorambucil breast cancers therapy. *J. Control Release* 274:56–68
- Lutz FT, Kianga S (2011) Prodrugs for targeted tumor therapies: recent developments in ADEPT, GDEPT and PMT. *Curr Pharm Design* 17:3527–3547
- Mahmudul H, Safaei A, Saikat Kumar P (2018) Antibody-drug conjugates: a review on the epitome of targeted anti-cancer therapy. *Curr Clin Pharmacol* 13:236–251
- Majzoub RN, Chan C-L, Ewert KK, Silva BFB, Liang KS, Jacovetty EL, Carragher B, Potter CS, Safinya CR (2014) Uptake and transfection efficiency of PEGylated cationic liposome–DNA complexes with and without RGD-tagging. *Biomaterials* 35:4996–5005
- Melwita E, Tsigie YA, Ismailji S, Ju Y-H (2011) Purification of azadirachtin via silica gel column chromatography. *J Liq Chromatogr Relat Technol* 34:2462–2472
- Mu L, Feng SS (2002) Vitamin E TPGS used as emulsifier in the solvent evaporation/extraction technique for fabrication of polymeric nanospheres for controlled release of paclitaxel (Taxol®). *J. Control Release* 80:129–144
- Mura S, Nicolas J, Couvreur P (2013) Stimuli-responsive nanocarriers for drug delivery. *Nat Mater* 12:991
- Nik ME, Malaekh-Nikouei B, Amin M, Hatamipour M, Teymour M, Sadeghnia HR, Irandshahi M, Jaafari MR (2019) Liposomal formulation of Galbanic acid improved therapeutic efficacy of pegylated liposomal doxorubicin in mouse colon carcinoma. *Sci Rep* 9:9527
- Oliyai R (1996) Prodrugs of peptides and peptidomimetics for improved formulation and delivery. *Adv Drug Deliver Rev* 19:275–286
- Petersen MA, Hillmyer MA, Kokkoli E (2013) Bioresorbable polymersomes for targeted delivery of cisplatin. *Bioconjjug Chem* 24:533–543
- Pirillo A, Catapano AL (2015) Berberine, a plant alkaloid with lipid- and glucose-lowering properties: from in vitro evidence to clinical studies. *Atherosclerosis* 243:449–461
- Sangrà M, Estelrich J, Sabaté R, Espargaró A, Busquets MA (2017) Evidence of protein adsorption in pegylated liposomes: influence of liposomal decoration. *Nanomaterials* 7:37
- Sapra P, Shor B (2013) Monoclonal antibody-based therapies in cancer: advances and challenges. *Pharmacol Therapeut* 138:452–469
- Shi K, Li J, Cao Z, Yang P, Qiu Y, Yang B, Wang Y, Long Y, Liu Y, Zhang Q, Qian J, Zhang Z, Gao H, He Q (2015) A pH-responsive cell-penetrating peptide-modified liposomes with active recognizing of integrin avβ3 for the treatment of melanoma. *J. Control Release* 217:138–150
- Tao X, Jia N, Cheng N, Ren Y, Cao X, Liu M, Wei D, Wang F-Q (2017) Design and evaluation of a phospholipase D based drug delivery strategy of novel phosphatidyl-prodrug. *Biomaterials* 131:1–14
- Wakaskar RR (2018) Promising effects of nanomedicine in cancer drug delivery. *J Drug Target* 26:319–324

- Wang Q, Zhang X, Liao H, Sun Y, Ding L, Teng Y, Zhu W-H, Zhang Z, Duan Y (2018) Multifunctional shell-core nanoparticles for treatment of multidrug resistance hepatocellular carcinoma. *Adv Funct Mater* 28:1706124
- Wu S, Wang Y, Gong G, Li F, Ren H, Liu Y (2015) Adsorption and desorption properties of macroporous resins for flavonoids from the extract of Chinese wolfberry (*Lycium barbarum* L.). *Food Bioprod Process* 93:148–155
- Xiang B, Dong D-W, Shi N-Q, Gao W, Yang Z-Z, Cui Y, Cao D-Y, Qi X-R (2013) PSA-responsive and PSMA-mediated multifunctional liposomes for targeted therapy of prostate cancer. *Biomaterials* 34:6976–6991
- Xiao Z, Levy-Nissenbaum E, Alexis F, Lupták A, Teply BA, Chan JM, Shi J, Digga E, Cheng J, Langer R, Farokhzad OC (2012) Engineering of targeted nanoparticles for cancer therapy using internalizing aptamers isolated by cell-uptake selection. *ACS Nano* 6:696–704
- Yang Y, Pan D, Luo K, Li L, Gu Z (2013) Biodegradable and amphiphilic block copolymer–doxorubicin conjugate as polymeric nanoscale drug delivery vehicle for breast cancer therapy. *Biomaterials* 34:8430–8443
- Yang Y, Yang Y, Xie X, Cai X, Zhang H, Gong W, Wang Z, Mei X (2014) PEGylated liposomes with NGR ligand and heat-activatable cell-penetrating peptide–doxorubicin conjugate for tumor-specific therapy. *Biomaterials* 35:4368–4381
- Zhang K, Wang X, Huang J, Liu Y (2012) Purification of l-alpha glycerophosphorylcholine by column chromatography. *J Chromatogr A* 1220:108–114
- Zheng X, Wu F, Lin X, Shen L, Feng Y (2018) Developments in drug delivery of bioactive alkaloids derived from traditional Chinese medicine. *Drug Deliv* 25:398–416
- Zhou H, Xu H, Li X, Lv Y, Ma T, Guo S, Huang Z, Wang X, Xu P (2017) Dual targeting hyaluronic acid—RGD mesoporous silica coated gold nanorods for chemo-photothermal cancer therapy. *Mater Sci Eng C Mater* 81:261–270
- Zhou C, Xie X, Yang H, Zhang S, Li Y, Kuang C, Fu S, Cui L, Liang M, Gao C, Yang Y, Gao C, Yang C (2019) Novel class of ultrasound-triggerable drug delivery systems for the improved treatment of tumors. *Mol Pharm* 16:2956–2965

Publisher's Note

Springer Nature remains neutral with regard to jurisdictional claims in published maps and institutional affiliations.